

*Original Research*

# Updating High-Resolution Emission Inventory to Unveil the Characteristics of Greenhouse Gases Emissions in Shandong Province, China

Ke Du<sup>1</sup>, Wei Jiang<sup>1,2\*</sup>, Weidong Gao<sup>1</sup>, Peng Song<sup>1</sup>, Xiao Ma<sup>1</sup>

<sup>1</sup>School of Water Conservancy and Environment, University of Jinan, Jinan, China

<sup>2</sup>College of Geography and Environment, Shandong Normal University, Jinan, China

*Received: 2 December 2022*

*Accepted: 7 March 2023*

## Abstract

Since stating carbon peak goal, Shandong has garnered widespread concern over its large GHG emissions. Based on the latest emission factors and detailed activity data, a comprehensive high-resolution GHG emission inventory of Shandong Province for 2020 was established by updating estimation methods and allocation profiles. The results indicated that the emissions of CO<sub>2</sub>, CH<sub>4</sub>, N<sub>2</sub>O, HFCs, PFCs and SF<sub>6</sub> had reached 1233.46, 36.49, 45.79, 74.27, 6.21 and 0.56 Mt CO<sub>2eq</sub>, respectively. Specifically, CO<sub>2</sub> emissions mainly originated from fossil fuel consumption (81.83%); the major sources of CH<sub>4</sub> emissions were mining industries and agriculture, contributing 1.40% and 0.81% of the total GHG emissions, respectively; industry processes and product use discharged the largest amount of N<sub>2</sub>O (1.92%) and were responsible for all of the fluorinated greenhouse gas emissions. To obtain more accurate GHG emission information, GHG emissions were spatially allocated to grid cells with a resolution of 0.05°×0.05° according to appropriate surrogates and results showed that most of the emissions are concentrated over a small number of grid cells, specifically, 10% of grid cells accounts for 73% of GHG, 75% of CO<sub>2</sub>, 88% of CH<sub>4</sub> and 40% of N<sub>2</sub>O emission. Spatially, the GHG emissions were mainly distributed in eastern and central cities of Shandong and decreased radially from urban centres to the surrounding areas.

**Keywords:** GHG emissions, high-resolution emission inventory, spatial distribution characteristics

## Introduction

The concentrations of carbon dioxide (CO<sub>2</sub>) and other greenhouse gases (GHGs) in the atmosphere quickly surged to their highest level in the last 800000 years and initiated a series of unprecedented

changes in the climate system in 2020 [1]. Due to its persistent economic growth and lifestyle changes, China, the world's largest developing country, surpassed the United States in 2006 to become the world's largest emitter of CO<sub>2</sub>, accounted for 27.3% of global GHG emissions in 2020 [2]. Rapidly increasing GHGs in the atmosphere has led to climate change, with negative impacts on nature, economics and society, and China has become one of the most

\*e-mail: stu\_Jiangw@ujn.edu.cn

severely affected regions in the world [3]. The Chinese government has had to reduce China's GHG emissions with enormous pressure and called for effective reduction actions. From signing the Kyoto Protocol at the Copenhagen Climate Conference 2009 to issuing "The Paris Agreement" in the United Nations in 2016, China has not only consistently promised to decrease its CO<sub>2</sub> emissions, but has also declared a series of medium-term and long-term development plans. The recently released Guideline for the 14<sup>th</sup> Five-Year Plan (2021-2026) stated a goal of "peak carbon emissions before 2030, carbon neutral before 2060" and control actions have been implemented nationwide [4]. Such intensified control actions show the determination of the Chinese government in promoting ecological civilization construction and transition to a sustainable society.

Continuous efforts to reduce GHG emissions in China have been made and scientists have paid greater attention to issues such as the development of a national GHG accounting system [5], GHG emission trends [6] and reduction targets [7], analysis of the causes of continued GHG growth [8], projections of future GHG emissions [9], the facilitating and inhibiting effects of urbanization on GHG emissions [10], and policy directions for reduction of GHG emissions [11]. These studies provided valuable data and theoretical support for policy-making and deepened the contents of GHG control. However, a knowledge gap still exists regarding identifying the key sources of GHG emissions and their contributions.

In recent years, with the establishment of stringent and concrete reduction targets for provincial and municipal governments, an emerging problem for local governments has been allocating the reduction responsibility of each sector and city to realize GHG reduction targets. A comprehensive emission inventory is the basis for formulating pertinent and scientific GHG emission control strategies. Although methods for establishing GHG emission inventories are relatively mature, they mainly focus on specific emission sources, such as energy [12], industry [9], agriculture [13], and transportation [14-15]. These methods have strongly pushed China's GHG emission inventories to become more sophisticated and dependable. Single emission source inventories can track the performance of each emission source and comprehensively reflect its characteristics; however, they cannot provide a holistic understanding of GHG emissions.

In terms of study regions, published studies have focused mainly on large, economically developed cities or hotspot regions with complete statistical data, such as Beijing [14], Shanghai [16], Tianjin [17], Chongqing [18], Nanjing [19] and Jinan [20]. Incomplete and unavailable data have hampered the precise estimation of GHG emissions and establishment of accurate city-level emission inventories for most other cities. Moreover, earlier studies focused mainly on CO<sub>2</sub>; some other GHG species, such as N<sub>2</sub>O, CH<sub>4</sub>, HFCs, PFCs and

SF<sub>6</sub>, which had greater global warming potentials and powerful impacts on climate, were much less discussed [21]. In addition, most studies did not consider the GHG sequestration of landscapes, which may lead to incomplete results in these inventories [22].

High-resolution emission inventories play a significant role in identifying the location and distribution of GHG emissions. However, due to the lack of detailed information about spatial distributions, it is difficult to describe the spatial characteristics of GHG emissions within an administrative unit. Following the methodology in the Guidelines for National Greenhouse Gas Inventories published by the Intergovernmental Panel on Climate Change [23], many countries and regions have attempted to establish high-resolution GHG emission inventories at national or global scales; existing inventories include: the Emissions Database for Global Atmospheric Research [24], Vulcan covering the USA and Canada, the European Monitoring and Evaluation Program [25], the China High Resolution Database [26], and the Multiscale Emissions Inventory Model for China [27]. Despite the acceptable spatial coverage capabilities, these emission maps have crude spatial resolutions (10 km×10 km or even lower) due to their enormous coverage area, and it is not possible to obtain sufficiently detailed data on the spatial patterns of GHG emissions for a particular administrative unit [28]. Moreover, considerable uncertainty in GHG spatial distribution still exists in mapping because of limited data sources [29].

In China, prefectural-level cities are the basic administrative units and the major carriers of energy consumption and GHG emissions, and they play an important role in achieving GHG reduction emission, however, their impact are rarely noticed and are poorly documented [30]. As the largest industrialized province with a large population in eastern China, Shandong was responsible for approximately 9% of China's GHG emissions [31]. Despite this, Shandong has not yet established an integrated and fine-grained high-resolution GHG emission inventory that hampers the local government from implementing an effective mitigation action plan. This paper aims to (1) establish a high-resolution GHG emission inventory (5 km × 5 km) at the Shandong Province city level for 2020 based on updating estimation methods and allocation profiles, including emissions of CO<sub>2</sub>, CH<sub>4</sub>, N<sub>2</sub>O, HFCs, PFCs, and SF<sub>6</sub>. This paper also aims to refine the classification of emission sources and employ more point source data and more appropriate spatial substitutions to improve the accuracy of the spatial distribution of GHG; (2) analyse GHG emission characteristics and regional inequity from multiple perspectives; (3) develop and present quantitative assessment methods for high-resolution emission inventories in relation to the uncertainty of activity data and emission factors and spatial data; and (4) provide a reference for GHG reduction actions for cities at different levels of development, which makes the inventory more universal and applicable. Compared

with previous studies this paper established a complete GHG emission inventory considering more sources (such as carbon sequestration from land use changes and forestry and fugitive emissions occurring in the coal mining) and more kinds of greenhouse gases (such as  $N_2O$ , HFCs, PFCs, and  $SF_6$ ), which make the estimation results more precise. In spatial allocation method, more point data based on field investigation was employed to improve the spatial accuracy.

## Data and Methodology

### Study Region and Inventory Boundaries

Shandong Province (sketching  $34^{\circ}22.9'N$  to  $38^{\circ}24.01'N$  and from  $114^{\circ}47.5'E$  to  $122^{\circ}42.3'E$ ) is located on the eastern coast of China and the estuary of the Yellow River, and had a population size of 101.72 million (rank second in China) and a GDP of 7312.9 billion yuan (rank third in China) in 2020 (Fig. 1). As a province dominated by heavy chemical industry, primary energy consumption of Shandong in 2020 reached 418.26 million ton standard coal equivalent (coal consumption accounted for 64%) and take about 9.18% of the national total. A large amount of fossil energy consumption and rapid economic development make it facing huge pressure for GHG reduction.

### Emission Estimation

Fine-grained source classification is the first and most important step in establishing a complete and correct emissions inventory [32]. Based on the latest literature [33], IPCC Guidelines [34] and Guidelines for Provincial Greenhouse Gas Inventories (for Trial Implementation) [35], the sources of emissions in this

paper were classified into three tiers. The first tiers distinguish 5 categories, including: Energy, Industry Processes and Product Use (IPPU), Agriculture, Forestry and Land Use Changes (FLUC), and Waste. The second and the third tiers further divides emission in each category into more detailed categories (Table S1). The main GHGs covered in this paper were carbon dioxide ( $CO_2$ ), methane ( $CH_4$ ), nitrous oxide ( $N_2O$ ), hydrofluorocarbons (HFCs), perfluorocarbons (PFCs), and sulfur hexafluoride ( $SF_6$ ), as specified in the Kyoto Protocol. To make it easier to compare GHGs, the emissions of six categories of GHGs were converted to carbon dioxide equivalent ( $CO_{2eq}$ ) emissions by multiplying their 100-year global warming potential coefficients, as proscribed in the Fifth Assessment Report of the IPCC [23].

As suggested by IPCC [34], GHGs (emissions and sequestration) emission can be estimated according to Equation (1):

$$E_{GHG} = \sum_i \sum_j \sum_k AD_{ijk} \times EF_{ijk} \quad (1)$$

Where  $E_{GHG}$  is the total GHG emissions,  $AD$  is the activity data, and  $EF$  is the emission factor,  $i$  is the GHG type ( $CO_2$ ,  $CH_4$ ,  $N_2O$ , HFCs, PFCs, and  $SF_6$ ),  $j$  is the GHG emission sector, and  $k$  is the technical types. It should be pointed that the estimation methods adopted in the actual process of inventory estimation vary slightly due to the characteristics of emission sources and availability of activity data.

To standardize the GHG emission estimation and to facilitate interregional comparability, 3 scopes were defined for the accounting and reporting of GHGs. All direct emissions within the Shandong Province administrative boundaries were considered to be Scope 1. The indirect emissions that exist beyond Shandong Province but are associated with Shandong Province's

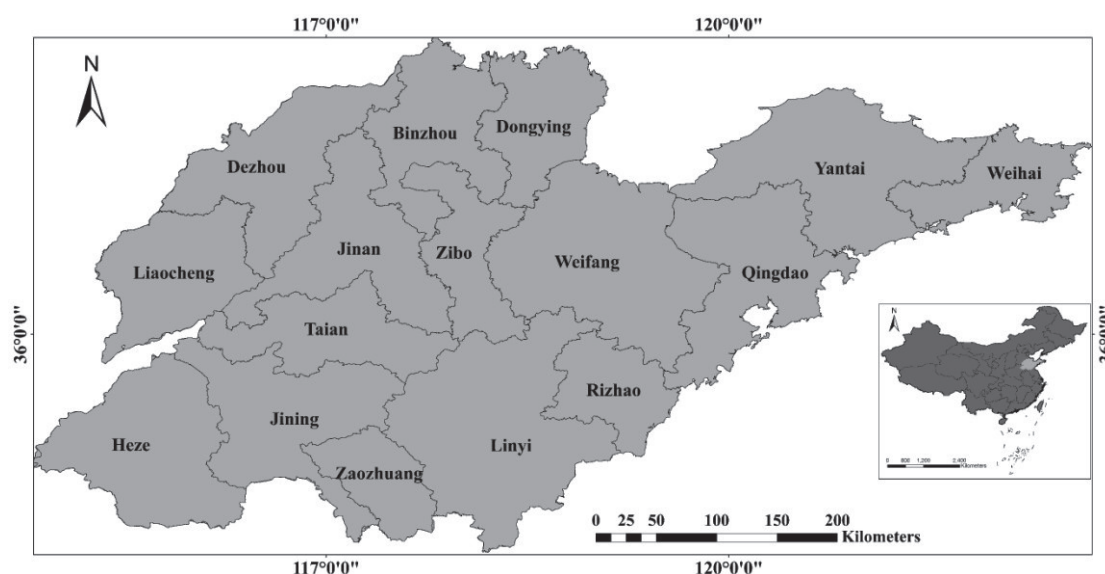


Fig. 1. Study domain and location.

energy activities were considered as Scope 2, mainly including inbound and outbound emissions of electricity and heat. Other types of indirect GHG emissions were considered to be Scope 3, such as energy losses. Waste generated in Shandong but disposed of outside Shandong was also considered as Scope 3. Accounting for both Scope 1 and Scope 2 is mandatory under most international GHG emissions reporting requirements.

### Spatial Allocation

In this paper, a 5 km × 5 km grid covering the entire Shandong province was created with ArcGIS software, with a total of 6509 grids. All emission sources were classified into three types according to their spatial characteristics: point, surface and line sources. To constrain the uncertainty, the emissions of each type of gas in the compiled GHG emissions inventory were assigned to a grid based on the emission characteristics of each source. For the key point sources (1952 units in total, Fig. S1) with specific geographical coordinates, such as power plants, heating plants, cement plants, steel plants, chemical plants (including adipic acid, nitric acid and HCFs production), sewage treatment plants, landfills and waste incineration plants, airports, ports, coal mines and oil wells, GHG emissions of these point sources were assigned to corresponding grid cells specifically based on their latitude and longitude. Among them, the amount of GHGs in each grid depended on the point source activity data. For other point sources without actual geographical coordinates available, their emissions were assigned to grid cells by surrogates that were similar to their actual geographical position and activity level, for example, the geographical positions of indoor burning and open burning were surrogated by rural residential areas and observational fire data from satellite [36], respectively. This method was also adopted in the spatial allocation of other emission sources, such as fossil fuel combustion of agriculture, forestry, animal husbandry and fishery. Line sources were mainly road mobile sources whose emissions were distributed into a grid according to the length of the road and type of road which is a popular method of moving source space allocation [37-38]. Other emission sources were ascribed to surface sources and were spatially assigned to a 0.05° × 0.05° grid by using specific spatial proxies as far as possible. For example, global nighttime lighting data and GDP data were used in a composite manner to make the spatial allocation of GHG emissions from the construction industry more accurate [39].

### Activity Data Collection

To guarantee the accuracy of the inventory, all activity data, which included information such as energy consumption, production output, land area, and population, were collected from official statistical data,

academic literature, and key enterprise investigation. For example, energy consumption data are from China Energy Statistical Yearbook 2021 [40]. Industrial economic data are from China Industry Statistical Yearbook 2021 and production data on key enterprises are from field investigation [41-42]. The emission factors used in this paper were mainly determined from relevant literature, the latest measured data of Shandong, and emission data of the surrounding province [30, 43-46]. Emission factors that conformed to Shandong's conditions were preferentially used. Sources of activity data and emission factors used in this paper are listed in Table S1.

For spatial allocation, detailed information on the latitude/longitude coordination of point sources was obtained from the Shandong Provincial Department of Ecology and Environment (<http://sthj.shandong.gov.cn/>) and Google Earth. The spatial proxy data selected for the line and surface sources were obtained from the Resource and Environment Science and the Data Centre (<https://www.resdc.cn/>). The spatial data used in this paper were defined in 4 levels (Table S2) based on the source, accuracy, consistency and fit of the data used for spatial allocation.

### Uncertainty Analysis

The uncertainty of GHG emission inventories mainly stems from defective and unfaithful data collection. In general, uncertainty analysis of inventories was mainly carried out with traditional Monte Carlo simulations, which put more emphasis on the uncertainty of emission factors and activity data as recommended by IPCC guidelines and pay little attention to the uncertainty of spatial distribution [47]. The establishment of a high-resolution GHG emissions inventory is a holistic process encompassing not only total emissions but also their spatial allocation, therefore, uncertainty estimates in this work were divided into uncertainty in emission inventories and uncertainty in spatial distribution. The uncertainty of the GHG emissions inventory was estimated using the Monte Carlo simulation method which is strongly recommended by the IPCC, and the error propagation method was used to estimate the uncertainty of the GHG spatial distribution. The Monte Carlo simulation process involves a large number of probability distributions and uncertainties in the emission factors and activity data parameters, which are described in detail in Table S3 and Table S4 [30, 48-50]. An uncertainty analysis approach for high-resolution emission inventories can be expressed as follows.

$$U = \sum U_{ADi} \times U_{EFi} \times U_{SAi} \times S_i \quad (2)$$

where  $U$  is the uncertainty of the high-resolution emissions inventory,  $U_{AD}$  is the uncertainty of the activity data,  $U_{EF}$  is the uncertainty of the emission factors,  $U_{SA}$  is the uncertainty of the spatial data,

$S$  is the proportion of emissions in the inventory estimated from the activity data, and  $i$  is GHG emissions type.

### Results and Discussion

#### Total GHG Emissions

The source-based GHG emission inventory in Shandong for year 2020 is summarized in Table S5. The total emissions of GHG were 1396.78 Mt CO<sub>2eq</sub>; emissions of CO<sub>2</sub>, CH<sub>4</sub>, N<sub>2</sub>O, HFCs, PFCs and SF<sub>6</sub> were 1233.46, 36.49, 45.79, 74.27, 6.21 and 0.56 Mt CO<sub>2eq</sub>, respectively. The main contribution of the major categories of GHG to the total emission is listed in Fig. 2 and Fig. S2. Fossil fuel combustion was the predominant contributor to GHG emissions (82.36%), and the main component of which is CO<sub>2</sub>, accounting for 81.83% of the total GHG emissions; mining industries and agriculture were the main emitter of CH<sub>4</sub>, accounting for 1.40% and 0.81% of the total GHG emissions, respectively; and IPPU and agriculture were the primary sources of N<sub>2</sub>O emissions, accounting for 1.92% and 0.85% of the total GHG emissions, respectively. Meanwhile, IPPU was the only observed source to HFCs, PFCs and SF<sub>6</sub>, accounted for 5.80%

of the total GHG emissions. In particular, HFCs, accounting for 5.32% of the total GHG emissions, overtook N<sub>2</sub>O and CH<sub>4</sub> to become the most influential greenhouse gas after CO<sub>2</sub>.

#### Energy Emissions

##### Fossil Fuel Consumption

Fossil fuel consumption was the largest source of GHG emissions, and mainly releases CO<sub>2</sub>, CH<sub>4</sub>, and N<sub>2</sub>O into the atmosphere. Because it is difficult to obtain detailed energy consumption data for each boiler, the GHG emissions from this sector were estimated according to the fossil fuel consumption data of the energy balance table and emission factors of each source.

The emissions of GHG from fossil fuel consumption reached 1150.38 Mt CO<sub>2eq</sub>, accounting for 82.36% of the total GHG emissions of Shandong. Specifically, Thermal power and heating supply as energy conversion sectors was the largest contributor to GHGs and produced 582.27 Mt CO<sub>2eq</sub> (41.69% of the total GHG emissions) due to Shandong's huge demand for electricity and heat. Industry as final energy consumption sectors contributed 268.52 Mt CO<sub>2eq</sub> (19.22% of the total GHG emissions) due to its huge energy consumption and

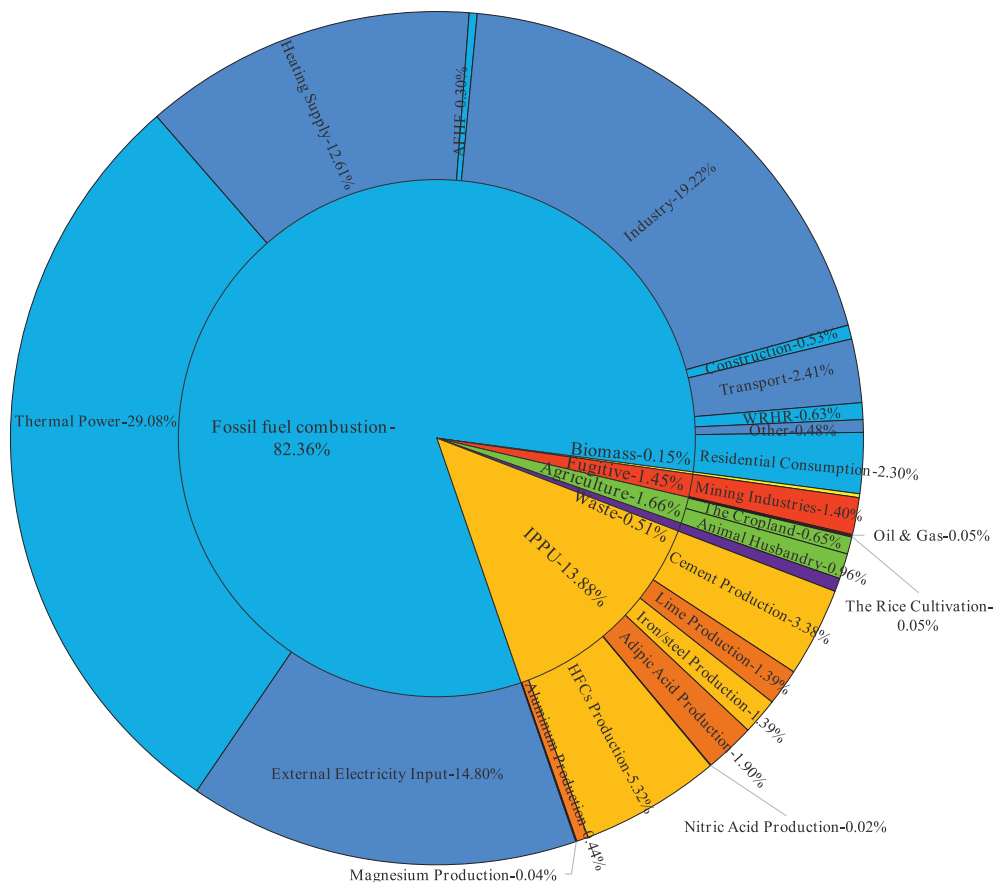


Fig. 2. The fractional contributions of major sectors to GHGs emissions in 2020 in Shandong.

coal-based energy structure. Residential consumption ranked third and produced 113.03 Mt CO<sub>2eq</sub> because of the large population of Shandong and modern lifestyle. Transport, storage, and postal services produced 42.39 Mt CO<sub>2eq</sub> due to the rapid growth of vehicles.

Effectuated by energy consumption structure of Shandong province, the GHG emission from different fossil fuels have varied greatly. As far as GHG emission from 27 energy types, the top six, namely raw coal, coke, blast furnace gas, diesel, natural gas and gasoline, accounted for 59.14% of total GHG emissions. In particular, GHG emissions came from raw coal combustion contributed 40.51% of total GHG emissions. Reducing energy consumption, especially raw coal consumption is vital in controlling GHG emission of Shandong province.

#### *Biomass Combustion*

Biomass energy of China is mainly used in household cooking and heating stoves or straw open burning, and release CH<sub>4</sub> and N<sub>2</sub>O during combustion process [51]. The amount of GHG emissions was estimated according to the crop economic production, grass-to-grain ratio, drying ratio, combustion efficiency, burning ratio and corresponding emission factors of different straw types [52-54]. Although Shandong province is a large agricultural province of China, the utilization of biomass energy is relatively low, and field investigations indicate that the indoor and open burning ratios of straw were 12.7% and 9.0% in 2020 [55]. The crops considered in this study include 18 crops such as wheat, rice and corn, which are widely grown in Shandong Province.

The GHG emissions from indoor burning (1.25 Mt CO<sub>2eq</sub>) and open burning (0.79 Mt CO<sub>2eq</sub>) was 0.15% of total GHG emissions of Shandong. Of all crops, GHG emissions from corn straw combustion reached 1.02 Mt CO<sub>2eq</sub> (49.89% of total biomass combustion) for the regional planting structure. Although straw burning is not the main body of GHG emissions, it releases a large amount of GHGs and gaseous pollutants; thus, it is regarded as an important source of air pollution and climate change in China. The Shandong government has issued the prohibition of open burning and pushed for the straw returning technique vigorously since 2013, however, the practice of open straw burning has continued to be performed secretly during harvest season because of insufficient profit. As a green, low-carbon, and economical renewable energy, biomass should be a viable replacement for fossil fuels that can achieve clean heating and effectively reduce air pollution and smog. But it had not achieved the desired effect due to the backward utilization technology and equipment of biomass [56]. Therefore, some monetary motivation, such as subsidy measures and new biomass stoves with more efficient installations, should be also provided to farmers to break the dilemma.

#### Fugitive Emissions

Fugitive emissions occurring in the coal mining (in the form of CH<sub>4</sub>) and oil and gas extraction process (in the form of CH<sub>4</sub> and CO<sub>2</sub>) significantly contributed to the emitted GHGs. A study has shown that CH<sub>4</sub> emissions from Chinese coal mines account for approximately one-third of CH<sub>4</sub> emissions each year, ranking first in the world [57]. The CH<sub>4</sub> emissions from coal mining in Shandong were estimated according to the coal mine production data from 190 mines (Fig. S1). Due to the difficulty in obtaining detailed data on the oil and gas supply chain, the GHG emissions of oil and gas fugitive emissions were estimated according to the oil and gas production data from 10 oil fields in Shandong and their update emission factors. The amount of fugitive emissions of CH<sub>4</sub> from coal mines in Shandong was 19.53 Mt CO<sub>2eq</sub>; this accounted for 53.54% of the total CH<sub>4</sub> emissions in Shandong in 2020, and the ratio was higher than the domestic average (38%) [58]. The main cause of the large emissions is that many coal mines in Shandong do not perform much CH<sub>4</sub> recovery. This implies that controlling of upstream emission can significantly and effectively reduce CH<sub>4</sub> emissions. Because of the technological improvement, emissions of CH<sub>4</sub> and CO<sub>2</sub> in the oil and gas sector were relatively low and only 0.69 and 0.02 Mt CO<sub>2eq</sub>.

Because CH<sub>4</sub> has a 28 times larger global warming potential than CO<sub>2</sub> and is mostly emitted into the atmosphere, it has become an important contributor to achieving carbon emission peaks. In recent years, technology for coalbed methane extraction and purification has made great developments, and its recovery rate and economic performance have improved significantly. The CH<sub>4</sub> released from coal mining and coalbeds can replenish China's scanty natural gas reserves and serve as an opportunity to reduce GHG emissions [59]. Therefore, the government should place greater emphasis on improving the current mining industry situation by encouraging integration with existing energy structures and markets.

#### Industry Processes and Product Use

The GHG emissions of IPPU refer to emissions from chemical reaction processes or physical change processes. The GHG emissions from IPPU were estimated according to industry production data of 684 large-scale industries (Fig. S1) and their emission factors. As an industrial province, Shandong displayed a complete range of industrial production, including 10 industrial processes that produce GHGs in this paper (Table S1).

The results indicate that the total CO<sub>2</sub>, N<sub>2</sub>O, HFCs, PFCs and SF<sub>6</sub> emissions from IPPU were 85.96, 26.85, 74.27, 6.21 and 0.56 Mt CO<sub>2eq</sub>, accounting for 6.15%, 1.92%, 5.32%, 0.44%, and 0.04% of the total GHG emissions of Shandong province, respectively. Cement production, lime production and steel production were

the CO<sub>2</sub> sources from IPPU, contributing 47.23, 19.37 and 19.35 Mt CO<sub>2eq</sub> of CO<sub>2</sub>, respectively. Popularizing the optimized production process and production equipment are effective approaches for IPPU to reduce CO<sub>2</sub> emission, for example, dry rotary kilns provide about 30% higher environmental benefit than shaft kilns for cement production [60]. As the major source of N<sub>2</sub>O emissions, adipic acid production contributed 26.56 Mt CO<sub>2eq</sub> of N<sub>2</sub>O, which was 1.90% of the total GHG emissions; PFCs (including CF<sub>4</sub> and C<sub>2</sub>F<sub>6</sub>) emissions that took place in aluminum production totalled 6.21 Mt CO<sub>2eq</sub>; and SF<sub>6</sub> emissions that took place in magnesium production totalled 0.56 Mt CO<sub>2eq</sub>; as the largest emitter of HFCs in industrial processes, HFCs production emitted 74.27 Mt CO<sub>2eq</sub> HFCs, accounting for 5.32% of the total GHG emissions due to the high demand for air conditioners and refrigerators. In addition, HFCs has already emitted more carbon equivalents than CH<sub>4</sub> and N<sub>2</sub>O and should be given more attention (Table S5).

### Agriculture

Agricultural GHG emissions include CH<sub>4</sub> and N<sub>2</sub>O. Specifically, CH<sub>4</sub> emissions mainly occur from rice planting, livestock enteric fermentation and livestock manure management; N<sub>2</sub>O emissions mainly occur in cropland and livestock manure management. The CH<sub>4</sub> emissions of this sector were estimated according to the rice planting area, the number of livestock and their corresponding emission factors. Cropland N<sub>2</sub>O emissions were estimated according to the use of fertilizer and maturity, the amount of straw returning, the crop area, the crop yield and their emission factors. Livestock N<sub>2</sub>O emissions were estimated according to the number of livestock and their emission factors.

As a major agricultural province of China, the amount of agricultural CH<sub>4</sub> and N<sub>2</sub>O emissions of Shandong reached 11.28 and 11.88 Mt CO<sub>2eq</sub>, contributing 0.81% and 0.85% of the total GHG emissions in 2020, respectively. In particular, the CH<sub>4</sub> emissions from livestock enteric fermentation reached 8.79 Mt CO<sub>2eq</sub>, 55.60% of which was from cattle (including dairy, non-dairy and buffalo), caused by their higher emission factor (cattle has three stomachs). The CH<sub>4</sub> emissions from livestock manure management reached 1.81 Mt CO<sub>2eq</sub>, 68.98% of which was from pigs due to their large population. In contrast, due to differences in planting structure, the rice planting area was only 1.06% of the Shandong planting area, and the CH<sub>4</sub> emissions were only 0.68 Mt CO<sub>2eq</sub>, accounting for 0.05% of the total GHG emissions.

Regarding N<sub>2</sub>O, the cropland emitted 9.06 Mt CO<sub>2eq</sub> of N<sub>2</sub>O, contributing 0.65% of the total GHG emissions, 47.19% of which was from fertilizer use. Because of the wide cultivation areas and overuse of fertilizer, corn and wheat planting accounted for 70.26% of the total emissions of all crops. The livestock manure management emitted 2.82 Mt CO<sub>2eq</sub> of N<sub>2</sub>O,

contributing 0.20% of the total GHG emissions. Poultry and pigs were the largest contributors due to their large populations, contributing 27.35% and 27.15% of the livestock manure management N<sub>2</sub>O emissions, respectively.

### Land Use Changes and Forestry

Forests can fix CO<sub>2</sub> in atmosphere into plant and soil through photosynthesis, being the main approach to decrease atmospheric CO<sub>2</sub>. LUCF are carbon sequestration sinks when the biomass from deforestation and destruction is less than the biomass added by forest growth. The amounts of carbon net sinks were estimated in this paper according to the total forest stock and their emission factor. To improve the accuracy of the estimation results, forestry in this paper was divided into 5 types, including arboreal forest, scattered tree, bamboo forest, economic forest and shrubbery.

The amount of CO<sub>2</sub> sequestration from forestry in Shandong Province reached 18.39 Mt CO<sub>2eq</sub>, the equivalent of 1.32% of the total GHG emissions in 2020. Arboreal forest contributed 38.93% of CO<sub>2</sub> sequestration (7.16 Mt CO<sub>2eq</sub>) and shrubbery were the main body of urban greening, contributing 36.46% of CO<sub>2</sub> sequestration (6.71 Mt CO<sub>2eq</sub>). As far as the real condition concerned, the CO<sub>2</sub> sequestration from forests is insufficient to offset the large amount of GHG emissions of Shandong province.

China is committed to reaching a carbon peak before 2030 and has put forth a set of carbon reduction actions in its 14<sup>th</sup> Five Year Plan. Forests and the soil carbon pool have a significant impact on the global carbon cycle in ecosystems, and mitigating climate change by planting forests and improving land use structures will be an effective way to reduce carbon emissions in the future.

### Waste

GHG emissions from the waste sector were composed of CH<sub>4</sub> emissions from landfill disposal, CO<sub>2</sub> emissions from solid waste incineration, and CH<sub>4</sub> and N<sub>2</sub>O emissions from domestic and industrial wastewater disposal. The amount of GHGs emissions from waste disposal was estimated according to waste disposal quantity (from 27 waste landfill plants, 36 waste incineration plants and 447 sewage disposal plants) (Fig. S1) and their emission factors.

As the most populated province in the eastern coastal region of China, Shandong has a very large waste production. GHG emissions from waste disposal reached 7.11 Mt CO<sub>2eq</sub> in 2020, accounting for 0.51% of the total GHG emissions. Compared to the disadvantage of landfill method in vegetation destruction and ground water pollution, waste incineration in a controlled manner can discharge less dangerous component and was widely adopted in Shandong. Then, CO<sub>2</sub> emissions

from waste incineration (3.88 Mt CO<sub>2eq</sub>) far exceeded the CH<sub>4</sub> emissions from waste landfills (0.72 Mt CO<sub>2eq</sub>), due to population and land pressure. The waste to electricity method is known as the best way to recycle, reduce and reuse solid waste. However, the waste incineration disposal ratio in Shandong was only 72.51% in 2020, and there was still a large gap compared to developed countries where the waste incineration disposal ratio was more than 80% [61].

Sewage disposal regulation and technology were already quite mature, the CH<sub>4</sub> emissions from domestic and industrial sewage disposal reached 0.62 Mt CO<sub>2eq</sub> and 0.05 Mt CO<sub>2eq</sub>, contributing 8.76% and 0.75% of the total waste disposal GHG emissions, respectively. Regarding N<sub>2</sub>O, domestic sewage disposal emitted 1.83 Mt CO<sub>2eq</sub> of N<sub>2</sub>O, contributing 25.76% of the total waste disposal GHG emissions. From the perspective of GHG emission reduction, the implementation of environmental protection fees and taxes could reduce waste output and help GHG emission reduction [62].

### Carbon Emissions Mapping

#### Spatial Distribution Pattern

Fig. 5 illustrates the spatial distributions of the GHG, CO<sub>2</sub>, CH<sub>4</sub> and N<sub>2</sub>O emissions. The GHG distribution have apparent spatial variability for the difference in industry structure and regions with high emission are found in middle and eastern cities. The CO<sub>2</sub> emission distribution is highly similar to that of GHG emissions because of its absolute contribution to GHG. For CO<sub>2</sub>, the grid cell areas with large emission intensities, which can also be called spatial emission intensities, were primarily concentrated in the eastern coastal and central

areas of Shandong Province and gradually decreased in a radial pattern from the centre areas of the cities to the surrounding areas. As the most vigorous port cities of the eastern coastal areas, Qingdao, Yantai, and Weihai have attracted a large population and advanced enterprises by virtue of their location and natural resources, and industrial agglomeration and household energy consumption resulted in more CO<sub>2</sub> emissions. As the traditional heavy industrial and transportation centre of Shandong Province, Jinan and Zibo also produce huge amounts of CO<sub>2</sub> emissions due to their large amount of energy consumption from many large petrochemical, metal smelting and cement enterprises. N<sub>2</sub>O was mainly concentrated in western Shandong Province due to the large area of arable land and intensive agricultural activities. High CH<sub>4</sub> emissions were mainly concentrated in southwestern Shandong where mining was densely located and have rich raw material processing industry.

To further delve into the characterization of GHGs spatial distribution, the paper counts GHGs emissions at grid criterion, whose probability distribution is shown in Fig. 4. The statistical results show that, most of the emissions are concentrated over a small number of grid cells, while the remaining large number of grid cells only account for a small part of the emissions. Specifically, 10% of grid cells accounts for 73% of GHG, 75% of CO<sub>2</sub>, 88% of CH<sub>4</sub> and 40% of N<sub>2</sub>O emission. However, the distribution of CO<sub>2</sub>, CH<sub>4</sub> and NO<sub>2</sub> have spatial inconsistency, that is the grid cell exceeding 75% of CO<sub>2</sub> emissions only contributed 24% of CH<sub>4</sub> emissions and 27% of N<sub>2</sub>O emissions.

The 0.05° × 0.05° spatial distribution of GHG emissions per unit of GDP and emissions per capita are displayed in Fig. 5. The grid cell areas with high GHG emissions per unit of GDP were mainly concentrated

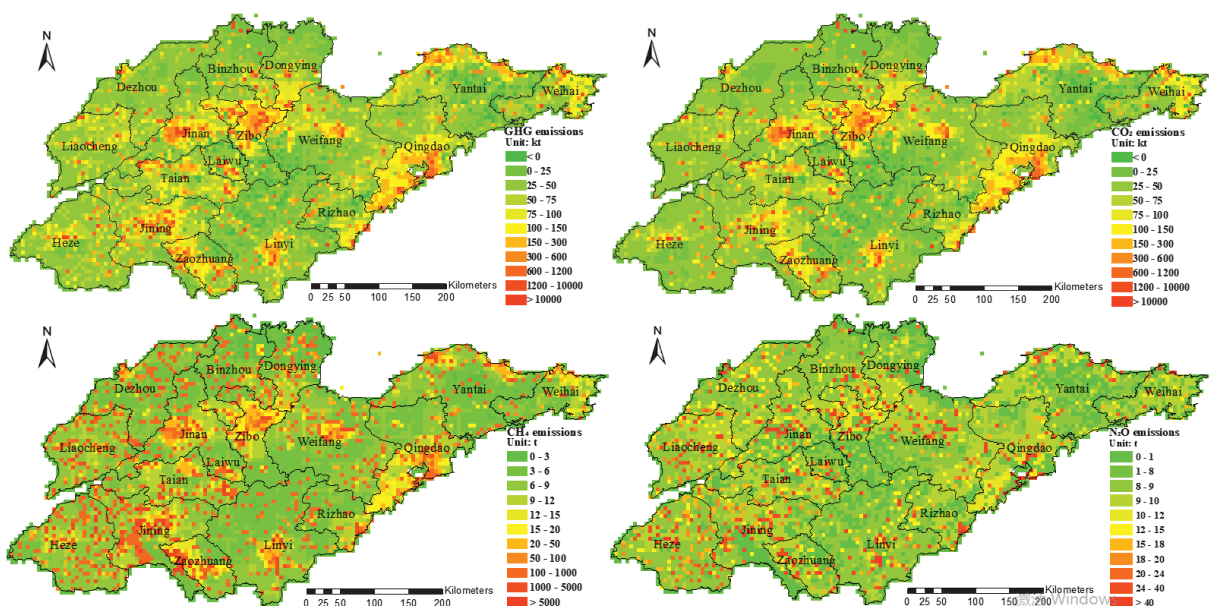


Fig. 3. Spatial distribution of GHG in the Shandong for the year 2020.

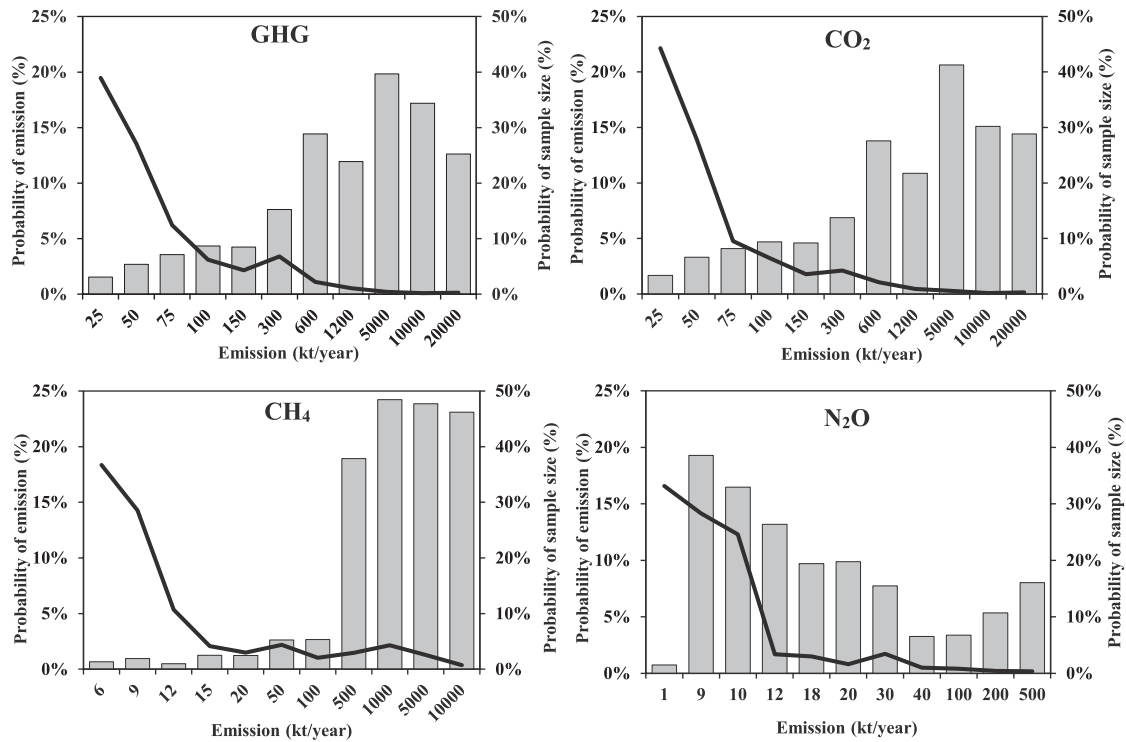


Fig. 4. The probability of GHGs emission amount over all grids in Shandong for 2020.

in western and southern Shandong Province. For cities of western Shandong Province, such as Heze and Liaocheng, the agricultural-based economic structure led to lower energy efficiency and economic output; thus, the economic emission intensity were relatively high. For cities in southern Shandong Province, such as Jining and Zaozhuang, the high economic emission intensity was mainly caused by the booming coal processing and coal electric industry, which consumed a large amount of coal. In contrast, in the eastern and northern cities of Shandong Province, the economic emission intensity was low due to their industrial agglomeration effect and upgraded industrial structure.

In terms of GHG emissions per capita, the grid cell areas with high values were mainly concentrated in the north and the middle south Shandong Province, where fuel guzzlers settled. The large amount of

energy consumption from these heavy industrial enterprises, such as Laiwu’s steel industry, Binzhou’s chemical industry and thermoelectric plants, Dongying’s petrochemical industry, Zibo’s equipment manufacturing industry and Zaozhuang’s coal-related industry have directly affected the GHG emissions per capita. In contrast, the population emission intensity of Jinan and Qingdao were low due to their rational industrial structure and the extensive application of clean energy technologies. The GHG emissions per capita of agricultural city, such as Heze, Liaocheng and Dezhou, were low due to their fewer major industries and less energy consumption. Meanwhile, the probability distribution (Fig. 6) indicates the emissions per GDP and the emissions per capita span a few orders, emphasizing the existence of large spatial inhomogeneity.

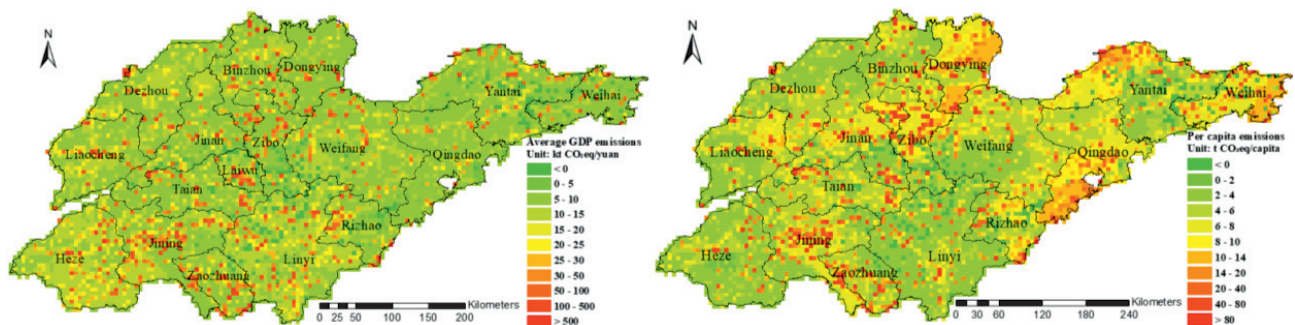


Fig. 5. Spatial distribution of GHG emission intensity in the Shandong for the year 2020.

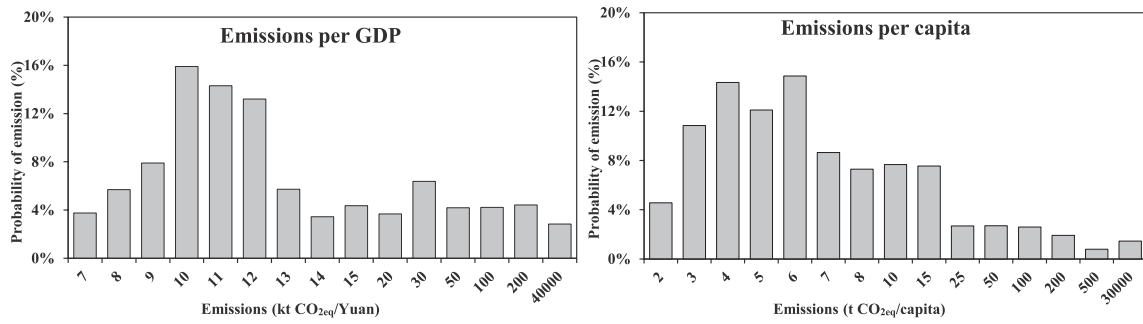


Fig. 6. Probability distributions of GHGs emissions per GDP and GHGs emissions per capita.

### Emissions Analysis by City

The Shandong GHG inventories at the city level are illustrated in Fig. 7. As the political and economic centres of Shandong, Jinan have become the largest GHG emitters of Shandong due to its developed industries, dense population and heavy traffic flows; its GHG emissions reached 131.00 Mt CO<sub>2eq</sub>, and contributed 9.37% of the total emissions. Qingdao come second because of its more developed low-carbon technologies. Jining had larger GHG emissions compared with the other industrialized cities due to the developed mining industry and energy industry. The GHG emissions in grid cell areas of Weifang were not prominent; however, small factors can add up to large numbers, so Weifang ranked fourth for its large number of machinery manufacturing factories. Therefore, for the sake of emission reduction fairness, the spatial emission intensity, economic emission intensity and population emission intensity should be synthetically considered in the process of clarifying the GHG emission responsibility.

The cities in Shandong Province can be classified into 4 categories according to their spatial emission intensity, economic emission intensity and population emission intensity (Fig. 8). The first group is cities with high economic emission intensity and high population

emission intensity, which include Zaozhuang, Zibo, Rizhao, Bingzhou and Laiwu. The large amount of primary energy consumption of energy-intensive enterprises in these cities, such as the steel industry of Rizhao and Laiwu, the thermoelectric plants of Binzhou and coal chemical industry and energy industry of Zaozhuang, and inefficient energy use is responsible for the gigantic GHG reduction potential of these cities. Accelerating industrial restructuring and vigorously developing high-tech industries and advanced manufacturing industries are effective ways to reduce the GHG contribution for these cities. The second group is cities with high population emission intensity and low economic emission intensity, which include Weihai and Dongying. Benefitting from their resource base and modern industry system, the economic emission intensity in this group is cut down. Current focus for these cities is reducing energy consumption and achieving low carbon of energy system. The third group is cities with high economic emission intensity and low population emission intensity, which includes all agricultural and coal mining cities in southern and western Shandong. Backwards production techniques cause cities in this group to face great emission reduction pressure, and industry restructuring will be crucial for carbon emission reduction. Industrial upgrading is the fundamental path to realize GHG

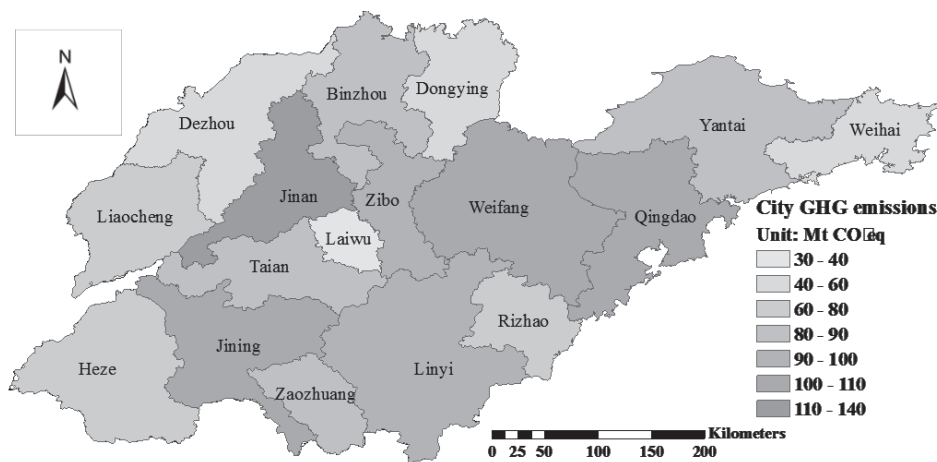


Fig. 7. Spatial distribution of the total GHG emission by city in the Shandong for the year 2020.

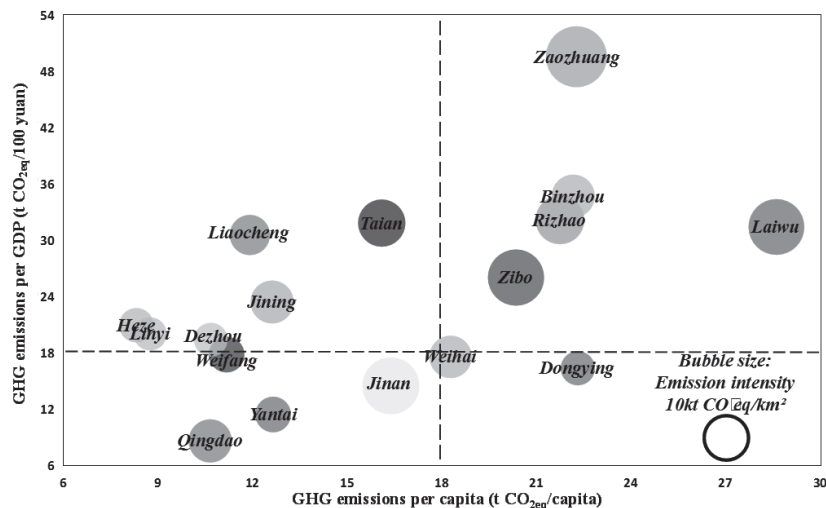


Fig. 8. Spatial emissions intensity ( $\text{kt CO}_{2\text{eq}}/\text{km}^2$ ), emissions per capita ( $\text{t CO}_{2\text{eq}}/\text{capita}$ ) and emissions per GDP ( $\text{t CO}_{2\text{eq}}/100$  yuan) of cities in the Shandong for the year 2020.

reduction for these cities. The fourth group includes cities with low economic emission intensity and low population emission intensity, which includes Qingdao, Jinan and Yantai. Cities of this group have a flourishing economy and reasonable industrial structure and energy efficiency are relatively high. As the leaders of regional development, technology innovation should be the important issue for them.

#### Uncertainty Analysis

The uncertainties in accounting for high-resolution GHG emissions inventories in this study consists mainly of the uncertainty in emission factors and activity data level as well as the uncertainty of spatial allocation.

After 10,000 Monte Carlo simulations with 95% confidence interval range, the average uncertainties of GHG emissions were -8 to 9% for  $\text{CO}_2$ , -35 to 45% for  $\text{CH}_4$ , -21 to 37% for  $\text{N}_2\text{O}$ , -46 to 47% for HFCs, -46 to 45% for PFCs and -56 to 32% for  $\text{SF}_6$ . The results show that the uncertainty of  $\text{CO}_2$  was relatively small because of comprehensive activity data and continuously updated emission factors. However, HFCs, PFCs and  $\text{SF}_6$  had larger uncertainties due to interview data and survey data were used in emissions estimates. The comprehensive uncertainty of [-21.63%, 25.24%] was obtained for the entire high-resolution GHG emissions inventory (Table S6), by adding uncertainties of spatial data to Monte Carlo simulations. One reason is the increase of point-emission source data from a maximum of 30% in the previous research to 57.39% in this study, which greatly reduced the influence of result's uncertainty. Moreover, by reducing the reliance on the spatial proxies that downscale city emissions to fine-scale grid cells, the spatial uncertainty in the distribution of emissions within a city was reduced significantly.

#### Conclusions

In this study, a high-resolution GHG emission inventory ( $0.05^\circ \times 0.05^\circ$ ) for Shandong in 2020 was performed based on updating estimation methods and allocation profiles. The total emissions of  $\text{CO}_2$ ,  $\text{CH}_4$ ,  $\text{N}_2\text{O}$ , HFCs, PFCs and  $\text{SF}_6$  were estimated to be 1233.46, 36.49, 45.79, 74.27, 6.21 and 0.56  $\text{Mt CO}_{2\text{eq}}$ , respectively.  $\text{CO}_2$  emissions largely came from fossil fuel consumption (especially from thermo-power plants), which contributed 82.36% of the total GHG emissions. Fugitive emissions from mining industries were the largest source of  $\text{CH}_4$  emissions, accounting for 1.40% of the total GHG emissions. Adipic acid production and cropland planting were determined to be the major sources of  $\text{N}_2\text{O}$  emissions, accounting for approximately 1.90% and 0.65% of the total GHG emissions, respectively. HFCs, PFCs and  $\text{SF}_6$  emissions, which came mainly from IPPU, such as refrigerant production, aluminum production and magnesium production, contributed 5.80% of the total emissions.

Spatially, the grid cell areas with large GHG emission were mainly concentrate in the in middle and eastern cities of Shandong Province because of population aggregation and industrial agglomeration. The grid cell areas with high population emission intensity were mainly concentrated in the north and the middle south of Shandong province where the fuel-guzzlers settled in. The grid cell areas with high economic emission intensity were mainly concentrated in western and southern Shandong Province for the lower energy efficiency and economic output.

According to spatial emission intensity, economic emission intensity and population emission intensity, the cities in Shandong Province are classified into four kinds: cities with high economic emission intensity and high population emission intensity, such as Zaozuang, Zibo, Rizhao, Binglezhou and Laiwu, accelerating

industrial restructuring and vigorously developing high-tech industries and advanced manufacturing industries are effective ways to reduce the GHG contribution for these cities. Cities with high population emission intensity and low economic emission intensity, such as Weihai and Dongying, current focus should put on reduce energy consumption and achieving low carbon of energy system. Cities in southern and western Shandong with high economic emission intensity and low population emission intensity, industry restructuring will be crucial for carbon emission reduction. Cities with low economic emission intensity and low population emission intensity, such as Qingdao, Jinan and Yantai, technology innovation should be the important issue for them.

Additionally, an extended method of uncertainty analysis was proposed to assess the uncertainty of inventories. And it was estimated that the uncertainty of this study got to be 22.15% for the entire high-resolution GHG emissions inventory. In the future, more attention should be paid to spatial uncertainty so that policy makers can more accurately know the spatial distribution of GHG emissions.

### Acknowledgments

This work was funded by the Natural Science Foundation of the Shandong Province (ZR2022MD010), the National Natural Science Foundation of China (21607054). The authors would like to thank the editors and anonymous referees for their valuable comments on an earlier version of this manuscript.

### Conflict of Interest

No conflict of interest exists in the submission of this manuscript, which has been approved by all authors for publication.

### References

- World Meteorological Organization. Available online: [https://library.wmo.int/doc\\_num.php?explnum\\_id=11352](https://library.wmo.int/doc_num.php?explnum_id=11352), 2021 (accessed on 6 May 2022).
- Energy Information Administration. Available online: <https://www.eia.gov/outlooks/ieo/index.php>, 2021 (accessed on 6 May 2022).
- XI F., GENG Y., CHEN X., ZHANG Y., WANG X., XUE B., DONG H., LIU Z., REN W., FUJITA T., ZHU Q. Contributing to local policy making on GHG emission reduction through inventorying and attribution: A case study of Shenyang, China. *Energy Policy*, **39** (10), 5999, 2011.
- National Development and Reform Commission. Available online: [https://www.ndrc.gov.cn/fggz/fzzlgh/gjzgh/202103/t20210323\\_1270102.html?code=&state=123](https://www.ndrc.gov.cn/fggz/fzzlgh/gjzgh/202103/t20210323_1270102.html?code=&state=123), 2021 (accessed on 6 May 2022).
- CHEN G.Q., CHEN Z.M. Carbon emissions and resources use by Chinese economy 2007: A 135-sector inventory and input-output embodiment. *Communications in Nonlinear Science and Numerical Simulation*, **15** (11), 3647, 2010.
- WANG Z.-X., YE D.-J. Forecasting Chinese carbon emissions from fossil energy consumption using non-linear grey multivariable models. *Journal of Cleaner Production*, **142**, 600, 2017.
- WANG S.J., FANG C.L., SUN L.X., SU Y.X., CHEN X.Z., ZHOU C.S., FENG K.S., HUBACEK K. Decarbonizing China's Urban Agglomerations. *Ann. Am. Assoc. Geogr.*, **109** (1), 266, 2019.
- DAI X.-W., SUN Z., MÜLLER D. Driving factors of direct greenhouse gas emissions from China's pig industry from 1976 to 2016. *Journal of Integrative Agriculture*, **20** (1), 319, 2021.
- LI S., ZHANG T., NIU L., YUE Q. Analysis of the development scenarios and greenhouse gas (GHG) emissions in China's aluminum industry till 2030. *Journal of Cleaner Production*, **290**, 125859, 2021.
- ZHANG C., LIN Y. Panel estimation for urbanization, energy consumption and CO<sub>2</sub> emissions: A regional analysis in China. *Energy Policy*, **49**, 488, 2012.
- ZENG L., XU M., LIANG S., ZENG S., ZHANG T. Revisiting drivers of energy intensity in China during 1997-2007: A structural decomposition analysis. *Energy Policy*, **67**, 640, 2014.
- LI J., WANG Y., XU D., XIE K. High-resolution analysis of life-cycle carbon emissions from China's coal-fired power industry: A provincial perspective. *International Journal of Greenhouse Gas Control*, **100**, 103110, 2020.
- HAN J., QU J., MARASENI T.N., XU L., ZENG J., LI H. A critical assessment of provincial-level variation in agricultural GHG emissions in China. *J Environ Manage*, **296**, 113190, 2021.
- LI Y., LV C., YANG N., LIU H., LIU Z. A study of high temporal-spatial resolution greenhouse gas emissions inventory for on-road vehicles based on traffic speed-flow model: A case of Beijing. *Journal of Cleaner Production*, **277**, 122419, 2020.
- GAO C., GAO C., SONG K., XING Y., CHEN W. Vehicle emissions inventory in high spatial-temporal resolution and emission reduction strategy in Harbin-Changchun Megalopolis. *Process Safety and Environmental Protection*, **138**, 236, 2020.
- LIU Z., LIANG S., GENG Y., XUE B., XI F., PAN Y., ZHANG T., FUJITA T. Features, trajectories and driving forces for energy-related GHG emissions from Chinese mega cites: The case of Beijing, Tianjin, Shanghai and Chongqing. *Energy*, **37** (1), 245, 2012.
- LAO J., SONG H., WANG C., ZHOU Y., WANG J. Reducing atmospheric pollutant and greenhouse gas emissions of heavy duty trucks by substituting diesel with hydrogen in Beijing-Tianjin-Hebei-Shandong region, China. *International Journal of Hydrogen Energy*, **46** (34), 18137, 2021.
- HU Y., YIN Z., MA J., DU W., LIU D., SUN L. Determinants of GHG emissions for a municipal economy: Structural decomposition analysis of Chongqing. *Applied Energy*, **196**, 162, 2017.
- BI J., ZHANG R., WANG H., LIU M., WU Y. The benchmarks of carbon emissions and policy implications for China's cities: Case of Nanjing. *Energy Policy*, **39** (9), 4785, 2011.

20. QI C., WANG Q., MA X., YE L., YANG D., HONG J. Inventory, environmental impact, and economic burden of GHG emission at the city level: Case study of Jinan, China. *Journal of Cleaner Production*, **192**, 236, **2018**.
21. LI Y., DU W., HUISINGH D. Challenges in developing an inventory of greenhouse gas emissions of Chinese cities: A case study of Beijing. *Journal of Cleaner Production*, **161**, 1051, **2017**.
22. ZHANG G., GE R., LIN T., YE H., LI X., HUANG N. Spatial apportionment of urban greenhouse gas emission inventory and its implications for urban planning: A case study of Xiamen, China. *Ecological Indicators*, **85**, 644, **2018**.
23. Intergovernmental Panel on Climate Change. Available online: <http://www.ipcc.ch/report/ar5/>. **2014** (accessed on 6 May 2022).
24. European Commission Joint Research Centre. Available online: <https://edgar.jrc.ec.europa.eu/>, **2016** (accessed on 6 May 2022).
25. SIMPSON D., BENEDICTOW A., BERGE H., BERGSTRÖM R., EMBERSON L.D., FAGERLI H., FLECHARD C.R., HAYMAN G.D., GAUSS M., JONSON J.E., JENKIN M.E., NYIRI A., RICHTER C., SEMEENA V.S., TSYRO S., TUOVINEN J.P., VALDEBENITO Á. and WIND P. The EMEP MSC-W chemical transport model – technical description. *Atmospheric Chemistry and Physics*, **12** (16), 7825, **2012**.
26. CAI B., LIANG S., ZHOU J., WANG J., CAO L., QU S., XU M., YANG Z. China high resolution emission database (CHRED) with point emission sources, gridded emission data, and supplementary socioeconomic data. *Resources, Conservation and Recycling*, **129**, 232, **2018**.
27. ZHENG B., CHENG J., GENG G., WANG X., LI M., SHI Q., QI J., LEI Y., ZHANG Q., HE K. Mapping anthropogenic emissions in China at 1 km spatial resolution and its application in air quality modeling. *Science Bulletin*, **66** (6), 612, **2021**.
28. CAI M., SHI Y. and REN C. Developing a high-resolution emission inventory tool for low-carbon city management using hybrid method – A pilot test in high-density Hong Kong. *Energy and Buildings*, **226**, 110376, **2020**.
29. HAN P., LIN X., ZENG N., ODA T., ZHANG W., LIU D., CAI Q., CRIPPA M., GUAN D., MA X., JANSSENS-MAENHOUT G., MENG W., SHAN Y., TAO S., WANG G., WANG H., WANG R., WU L., ZHANG Q., ZHAO F., ZHENG B. Province-level fossil fuel CO<sub>2</sub> emission estimates for China based on seven inventories. *Journal of Cleaner Production*, **277**, 123377, **2020**.
30. CAI B., CUI C., ZHANG D., CAO L., WU P., PANG L., ZHANG J., DAI C. China city-level greenhouse gas emissions inventory in 2015 and uncertainty analysis. *Applied Energy*, **253**, 113579, **2019**.
31. ZHAO Y., NIELSEN C.P., MCELROY M.B. China's CO<sub>2</sub> emissions estimated from the bottom up: Recent trends, spatial distributions, and quantification of uncertainties. *Atmospheric Environment*, **59**, 214, **2012**.
32. ZHOU M., JIANG W., GAO W., ZHOU B., LIAO X. A high spatiotemporal resolution anthropogenic VOC emission inventory for Qingdao City in 2016 and its ozone formation potential analysis. *Process Safety and Environmental Protection*, **139**, 147, **2020**.
33. GAO Y., ZHANG L., HUANG A., KOU W., BO X., CAI B., QU J. Unveiling the spatial and sectoral characteristics of a high-resolution emission inventory of CO<sub>2</sub> and air pollutants in China. *Sci Total Environ*, **847**, 157623, **2022**.
34. Intergovernmental Panel on Climate Change. Available online: <http://www.ipcc-nggip.iges.or.jp/public/gl/invs1.html>, **2006** (accessed on 6 May 2022).
35. National Development and Reform Commission. Available online: <http://www.cbcsd.org.cn/sjk/nengyuan/standard/home/20140113/download/shengjiwenshiqiti.pdf>, **2011** (accessed on 6 May 2022).
36. SHI Y., GONG S., ZANG S., ZHAO Y., WANG W., LV Z., MATSUNAGA T., YAMAGUCHI Y., BAI Y. High-resolution and multi-year estimation of emissions from open biomass burning in Northeast China during 2001-2017. *Journal of Cleaner Production*, **310**, 127496, **2021**.
37. HAKKIM H., KUMAR A., ANNADATE S., SINHA B., SINHA V. RTEII: A new high-resolution (0.1° × 0.1°) road transport emission inventory for India of 74 speciated NMVOCs, CO, NO<sub>x</sub>, NH<sub>3</sub>, CH<sub>4</sub>, CO<sub>2</sub>, PM<sub>2.5</sub> reveals massive overestimation of NO<sub>x</sub> and CO and missing nitromethane emissions by existing inventories. *Atmospheric Environment: X*, **11**, 100118, **2021**.
38. SINGH V., SAHU S.K., KESARKAR A.P., BISWAL A. Estimation of high resolution emissions from road transport sector in a megacity Delhi. *Urban Climate*, **26**, 109, **2018**.
39. LI P., ZHANG H., WANG X., SONG X., SHIBASAKI R. A spatial finer electric load estimation method based on night-light satellite image. *Energy*, **209**, 118475, **2020**.
40. National Bureau of Statistics of China. Available online: **2021** (accessed on 6 May 2022).
41. Ministry of Ecology and Environment of the People's Republic of China. Available online: <http://fb.sdem.org.cn:8801/zxjc/index.htm>, **2021** (accessed on 6 May 2022).
42. SHAN Y., LIU Z., GUAN D. CO<sub>2</sub> emissions from China's lime industry. *Applied Energy*, **166**, 245, **2016**.
43. LI L., YANG J. A new method of energy-related carbon dioxide emissions estimation at the provincial-level: A case study of Shandong Province, China. *Sci Total Environ*, **700**, 134384, **2020**.
44. Office of the Coordination Group on national Climate change responses. Available online: **2007** (accessed on 6 May 2022).
45. Office of the Coordination Group on national Climate change responses. Available online: **2014** (accessed on 6 May 2022).
46. GENG Y., TIAN M., ZHU Q., ZHANG J., PENG C. Quantification of provincial-level carbon emissions from energy consumption in China. *Renewable and Sustainable Energy Reviews*, **15** (8), 3658, **2011**.
47. SHAN Y., GUAN D., LIU J., MI Z., LIU Z., LIU J., SCHROEDER H., CAI B., CHEN Y., SHAO S., ZHANG Q. Methodology and applications of city level CO<sub>2</sub> emission accounts in China. *Journal of Cleaner Production*, **161**, 1215, **2017**.
48. GRIGGS D.J., NOGUER M. Climate change 2001: The scientific basis. Contribution of Working Group I to the Third Assessment Report of the Intergovernmental Panel on Climate Change. *Weather*, **57** (8), 267, **2002**.
49. WINIWARTER W., MUIK B. Statistical dependence in input data of national greenhouse gas inventories: effects on the overall inventory uncertainty. *Climatic Change*, **103** (1-2), 19, **2010**.
50. YAN F., WINIKUL E., BOND T.C., STREETS D.G. Global emission projections of particulate matter (PM): II. Uncertainty analyses of on-road vehicle exhaust emissions. *Atmospheric Environment*, **87**, 189, **2014**.

51. WANG Y.-J., BI Y.-Y., GAO C.-Y. The Assessment and Utilization of Straw Resources in China. *Agricultural Sciences in China*, **9** (12), 1807, **2010**.
52. SHARMA A., SINGH G., ARYA S.K. Biofuel from rice straw. *Journal of Cleaner Production*, **277**, 124101, **2020**.
53. GAO R., JIANG W., GAO W., SUN S. Emission inventory of crop residue open burning and its high-resolution spatial distribution in 2014 for Shandong province, China. *Atmospheric Pollution Research*, **8** (3), 545, **2017**.
54. CUI S., SONG Z., ZHANG L., SHEN Z., HOUGH R., ZHANG Z., AN L., FU Q., ZHAO Y., JIA Z. Spatial and temporal variations of open straw burning based on fire spots in northeast China from 2013 to 2017. *Atmospheric Environment*, **244**, 117962, **2021**.
55. WANG S., FENG H., ZOU B., YANG Z., DING Y. Correlation between biomass burning and air pollution in China: Spatial heterogeneity and corresponding factors. *Global and Planetary Change*, **213**, 103823, **2022**.
56. SONG C., HE J., ZHANG H. Comprehensive zoning of biomass energy heating in EU countries reference for China from European experience. *Chinese Journal of Population, Resources and Environment*, **19** (4), 321, **2021**.
57. GAO J., GUAN C., ZHANG B. China's CH<sub>4</sub> emissions from coal mining: A review of current bottom-up inventories. *Sci Total Environ*, **725**, 138295, **2020**.
58. MA C., DAI E., LIU Y., WANG Y., WANG F. Methane fugitive emissions from coal mining and post-mining activities in China. *Resources Science*, **42** (2), 311, **2020**.
59. SINGH A.K., KUMAR J. Fugitive Methane Emissions from Indian Coal Mining and Handling Activities: Estimates, Mitigation and Opportunities for its Utilization to Generate Clean Energy. *Energy Procedia*, **90**, 336, **2016**.
60. CHEN W., HONG J., XU C. Pollutants generated by cement production in China, their impacts, and the potential for environmental improvement. *Journal of Cleaner Production*, **103**, 61, **2015**.
61. YANG Y., LU X., JIANG J., MA J., LIU G., CAO Y., LIU W., LI J., PANG S., KONG X., LUO C. Degradation of sulfamethoxazole by UV, UV/H<sub>2</sub>O<sub>2</sub> and UV/persulfate (PDS): Formation of oxidation products and effect of bicarbonate. *Water Res*, **118**, 196, **2017**.
62. TRIYONO B., PRAWISUDHA P., AZIZ M., MARDIYATI, PASEK A.D., YOSHIKAWA K. Utilization of mixed organic-plastic municipal solid waste as renewable solid fuel employing wet torrefaction. *Waste Manag*, **95**, 1, **2019**.

## Supplementary Material

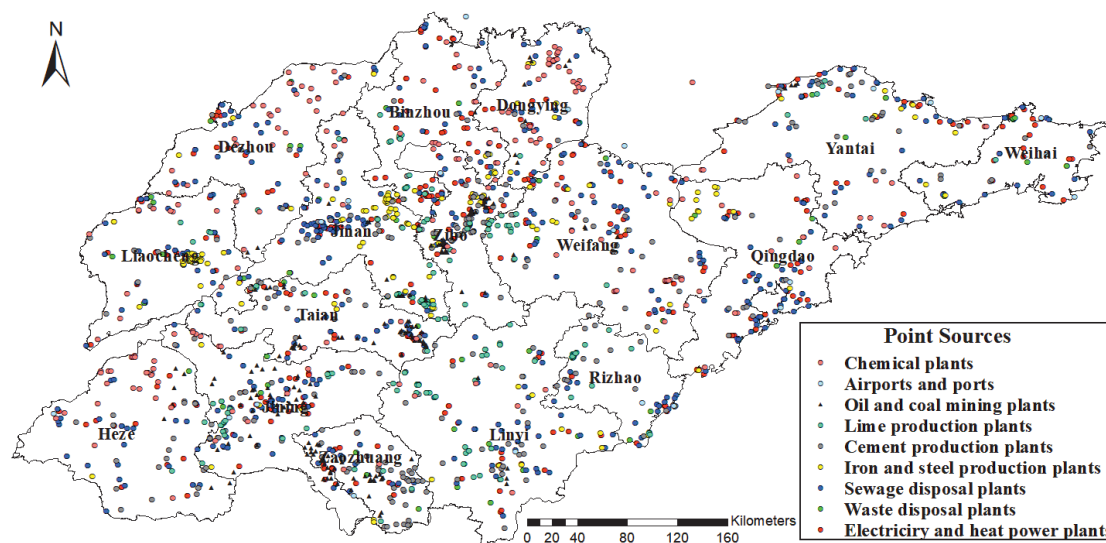


Fig. S1. Location of key point sources in the Shandong province.

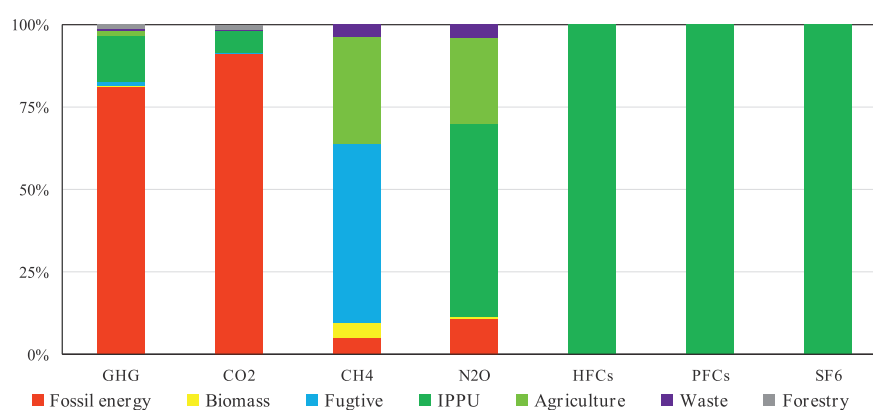


Fig. S2. Emission contributions by sector in the Shandong for the year.

Table S1. GHG emission sources classification and data source.

The first tier	The second tier	The third tier	Source
Energy	Fossil fuel combustion	Thermal Power	China Energy Statistical Yearbook, Shandong Statistical Yearbook, Department of Ecological Environment of Shandong Province and Ministry of Ecology and Environment of the People's Republic of China.
		Heating Supply	
		Agriculture, Forestry, Husbandry and Fishery	
		Industry	
		Construction	
		Transport, Storage and Post	
		Wholesale, Retail Trade and Hotel, Restaurants	
		Residential Consumption	
	Biomass burning	Indoor burning	Shandong Statistical Yearbook and Literature.
		Open burning	
Fugitive emission	Fugitive emissions of mining industries	Shandong Statistical Yearbook, Literature Governmental reports and Production licenses.	
	Fugitive emissions of oil & gas		
Industry processes and product use		Cement Production	China Industry Economy Statistical Yearbook, Shandong Statistical Yearbook, Department of Ecological Environment of Shandong Province and Ministry of Ecology and Environment of the People's Republic of China.
		Lime Production	
		Iron/steel Production	
		Calcium Carbide	
		Adipic Acid Production	
		Nitric Acid Production	
		HCFC-22 Production	
		Aluminum Production	
		Magnesium Production	
HCFs Production			
Agriculture		CH <sub>4</sub> emission from the rice cultivation	China Animal Husbandry and Veterinary Yearbook and Shandong Statistical Yearbook.
		N <sub>2</sub> O emission from the cropland	
		Enteric fermentation and manure management	
Waste disposal	Waste	Waste Landfill	China Urban Construction Statistical Yearbook
		Waste Incineration	
	Wastewater	Household Wastewater	
		Industry Wastewater	

Table S1. Continued.

Land use changes and forestry	Forest and other woody biomass carbon stock	China Forestry Statistical Yearbook and the ninth National Forest Inventory.
	Forest land conversion	

Table S2. Spatial allocation types and their uncertainty levels.

Level	Accuracy	
A	95%	Actual geographic data, without any spatial agents
B	90%	Spatial agents associated with actual data
C	80%	Spatial agents that are directly related to the actual data
D	70%	Spatial agents that are indirectly related to the actual data

Table S3. Emission factor parameter uncertainty and probability distribution.

Activity department	Emission factor related parameters	Uncertainty	Probability distribution type
Fossil fuel combustion	CO <sub>2</sub>	7%	Normal
	CH <sub>4</sub>	-50%-150%	Lognormal
	N <sub>2</sub> O	-70%-150%	Lognormal
Biomass burning	CH <sub>4</sub>	16.5%	Uniform
	N <sub>2</sub> O	20%	Uniform
Fugitive emission	Key State-owned	-80%-130%	Lognormal
	Local State-owned	-80%-140%	Lognormal
	Town-owned	-80%-150%	Lognormal
IPPU	Cement Production	2%	Normal
	Lime Production	2%	Normal
	Iron/steel Production	25%	Normal
	Calcium Carbide	5%	Normal
	Adipic Acid Production	10%	Normal
	Nitric Acid Production	20%	Normal
	HCFC-22 Production	10%	Normal
	Aluminum Production	50%	Normal
	Magnesium Production	60%	Normal
HCFs Production	50%	Normal	
Agriculture	Rice cultivation	35%	Normal
	Cropland indirect emission	0.0258-0.0021	Triangular
	Cropland direct emission	0.01-0.002	Triangular
	Intestinal fermentation	30%	Normal
	Manure management CH <sub>4</sub>	20%	Normal
	Manure management N <sub>2</sub> O	-50%-100%	Lognormal
LUCF	Growing stock volume growth rate	10%	Normal
	Consumption rate of stock volume	10%	Normal
	Weighted average of wood density	12%	Normal
	Biomass conversion factor	12.5%	Normal

Table S3. Continued.

Waste	CH <sub>4</sub> correction factor	30%	Normal
	DOC content ratio	10%	Normal
	Decomposable DOC ratio	20%	Normal
	CH <sub>4</sub> Proportion in Landfill Gas	5%	Normal
	Domestic sewage CH <sub>4</sub> emission	5%	Normal
	Protein nitrogen content	30%	Normal
	Industrial sewage CH <sub>4</sub> emission	15%	Normal

Other data without a superscript are based on IPCC [1], the national GHG inventory [2] and experts' advice.

Table S4. Active data parameter uncertainty and probability distribution.

Activity department	Activity data related parameters	Uncertainty	Probability distribution type
Energy	Electric heat production	3%	Normal
	Business and Residents combustion	3%	Normal
	Industrial burning	2%	Normal
	Construction consumption	3%	Normal
	Transportation consumption	15.00% <sup>a</sup>	Normal
	Biomass combustion	10%	Normal
	Fugitive coal	15%	Normal
	Fugitive Oil and Natural Gas	5%	Normal
IPPU	Cement Production	1%	Normal
	Lime Production	4%	Normal
	Iron/steel Production	10%	Normal
	Calcium Carbide	5%	Normal
	Adipic Acid Production	2%	Normal
	Nitric Acid Production	2%	Normal
	HCFC-22 Production	5%	Normal
	Aluminum Production	1%	Normal
	Magnesium Production	20%	Normal
	HCFs Production	30%	Normal
Agriculture	Crop Area	9%	Normal
	Livestock population	20%	Normal
LUCF	living wood growing stock	3%	Normal
Waste	Waste Composition	10%	Normal
	Sewage treatment capacity	12%	Normal

Other data without a superscript are based on the national GHG inventory and experts' advice [3-4].

Table S5. GHG emission inventory data (Unit: Mt CO<sub>2eq</sub>).

Sector	Sub	CO <sub>2</sub>	CH <sub>4</sub>	N <sub>2</sub> O	HFCs	PFCs	SF <sub>6</sub>	GHG	Total
Energy	Fossil fuel consumption	<b>1143.61</b>	1.89	4.89				1150.38	1172.66
	Biomass combustion		1.71	0.34				2.04	
	Fugitive emissions of mining industries		19.53					19.53	
	Fugitive emissions of oil & gas	0.02	0.69					0.71	
IPPU	IPPU	85.96		<b>26.85</b>	<b>74.27</b>	<b>6.21</b>	<b>0.56</b>	193.85	193.85
Agriculture	Rice cultivation		0.68					0.68	23.16
	Cropland planting			9.06				9.06	
	Livestock enteric fermentation and manure		10.60	2.82				13.42	
Waste	Waste Landfill		0.72					0.72	7.10
	Waste Incineration	3.88						3.88	
	Household Wastewater		0.62	1.83				2.45	
	Industry Wastewater		0.05					0.05	
Total		1233.46	36.49	45.79	74.27	6.21	0.56		1396.78
LUCF	Forestry	-18.39						-18.39	-18.39

Table S6. The uncertainty high-resolution GHG emissions inventory.

a). Uncertainties of emission inventory by sector for Shandong in 2020.

Category	CO <sub>2</sub>	CH <sub>4</sub>	N <sub>2</sub> O	HFCs	PFCs	SF <sub>6</sub>	GHG
Industry energy consumption	-7% - 7%	-47% - 156%	-60% - 107%				-8% - 9%
Agriculture energy consumption	-8% - 8%	-47% - 156%	-60% - 118%				-9% - 11%
Construction energy consumption	-7% - 7%	-47% - 150%	-61% - 142%				-8% - 8%
Transport energy consumption	-16% - 17%	-47% - 113%	-61% - 148%				-17% - 18%
Residential energy consumption	-8% - 8%	-47% - 166%	-59% - 104%				-10% - 12%
Wholes energy consumption	-9% - 9%	-47% - 143%	-47% - 118%				-9% - 9%
Other energy consumption	-9% - 9%	-46% - 136%	-59% - 84%				-10% - 10%
biomass burning		-52% - 32%	-17% - 15%				-25% - 52%
Fugitive emissions	-12% - 11%	-39% - 48%					-39% - 48%
IPPU	-6% - 6%		-17% - 17%	-46% - 47%	-46% - 45%	-56% - 32%	-23% - 30%
Agriculture activity		-29% - 35%	-18% - 41%				-23% - 39%
Waste disposal	-32% - 86%	-30% - 38%	-28% - 28%				-30% - 48%
Forest	-16% - 17%						-16% - 17%
Total	-8% - 9%	-35% - 45%	-21% - 37%	-46% - 47%	-46% - 45%	-56% - 32%	-13% - 14%

Table S6. The uncertainty high-resolution GHG emissions inventory.

b) The uncertainty of high-resolution GHG emissions inventory by sector for Shandong in 2020.

Sub-category	Activity data description	Space type	Spatial surrogates	Space uncertainty <sup>a</sup>	Inventory uncertainty <sup>b</sup>	Share <sup>c</sup>
Fossil fuel combustion	Thermal Power	Point	Actual geographic position	95%	[92.17%, 108.55%]	28.70%
	Heating Supply	Point	Actual geographic position	95%	[91.74%, 108.89%]	12.45%
	Agriculture, Forestry, Husbandry and Fishery	Point	Rural residential area	80%	[90.54%, 111.31%]	0.47%
	Industry	Surface	GDP distribution data	80%	[91.95%, 108.54%]	30.69%
	Construction	Surface	Global night light data, GDP distribution data	70%	[92.22%, 108.38%]	0.63%
	Transport, Storage and Post	Line	Road network	90%	[82.99%, 117.79%]	2.54%
	Wholesale, Retail Trade and Hotel, Restaurants	Surface	GDP distribution data	70%	[91.20%, 109.46%]	0.94%
	Residential Consumption	Surface	Population density	80%	[90.34%, 111.98%]	4.87%
Biomass burning	Indoor burning	Point	Rural residential area	80%	[50.74%, 126.41%]	0.09%
	Open burning	Point	The fire data	90%	[82.46%, 117.14%]	0.06%
Fugitive emission	Fugitive emissions of mining industries	Point	Actual geographic position	95%	[60.35%, 148.59%]	1.38%
	Fugitive emissions of oil & gas	Point	Actual geographic position	95%	[93.93%, 107.04%]	0.05%
IPPU	Cement Production	Point	Actual geographic position	95%	[98.10%, 102.21%]	3.34%
	Lime Production	Point	Actual geographic position	95%	[96.10%, 103.78%]	1.37%
	Iron/steel Production	Point	Actual geographic position	95%	[75.81%, 125.04%]	1.37%
	Calcium Carbide	Point	Actual geographic position	95%	[0%,0%]	0.00%
	Adipic Acid Production	Point	Actual geographic position	95%	[82.06%, 118.23%]	1.88%
	Nitric Acid Production	Point	Actual geographic position	95%	[90.15%, 110.13%]	0.02%
	HCFC-22 Production	Point	Actual geographic position	95%	[53.89%, 146.95%]	5.13%
	Aluminum Production	Point	Actual geographic position	95%	[53.88%, 144.79%]	0.44%
	Magnesium Production	Point	Actual geographic position	95%	[43.86%, 131.58%]	0.04%
	HCFs Production	Point	Actual geographic position	95%	[52.16%, 151.72%]	0.11%
Agriculture	CH <sub>4</sub> emission from the rice cultivation	Surface	Land type map	90%	[90.76%, 109.06%]	0.05%
	N <sub>2</sub> O emission from the cropland	Surface	Cultivated land area	90%	[94.53%, 125.20%]	0.64%
	enteric fermentation and manure management	Surface	Rural residential area	80%	[64.32%, 149.69%]	0.95%
Waste	Waste Landfill	Point	Rural residential area	95%	[68.36%, 136.50%]	0.05%
	Waste Incineration	Point	Rural residential area	95%	[67.95%, 185.59%]	0.27%

Table S6. b) Continued.

Wastewater	Household Wastewater	Point	Rural residential area	95%	[71.86%, 128.10%]	0.17%
	Industry Wastewater	Point	Rural residential area	95%	[73.60%, 128.80%]	0.00%
FLUC	Forest and woody biomass carbon stock	Surface	Vegetation map	90%	[84.10%, 117.45%]	1.30%
	Forest land conversion	Surface	Land type map	90%	[0%,0%]	28.70%
Total					[87.21%, 114.36%] <sup>d</sup> [78.37%, 125.24%] <sup>e</sup>	

<sup>a</sup> The uncertainty value was calculated by the author without probability distribution calculation, but it can be used for peer evaluation.

<sup>b</sup> Interval of uncertainty derived from Monte Carlo simulation.

<sup>c</sup> The new share, which add the absolute value of carbon sink and the out of boundary electricity was distributed to final energy consumption.

<sup>d</sup> The comprehensive uncertainties of GHG emission inventory, which did not add uncertainties of spatial data.

<sup>e</sup> The comprehensive uncertainty of the high-resolution GHG emission inventory, which add uncertainties of spatial data.

### References

- GRIGGS D.J., NOGUER M. Climate change 2001: The scientific basis. Contribution of Working Group I to the Third Assessment Report of the Intergovernmental Panel on Climate Change. *Weather*, **57** (8), 267, **2002**.
- CAI B., CUI C., ZHANG D., CAO L., WU P., PANG L., ZHANG J., DAI C. China city-level greenhouse gas emissions inventory in 2015 and uncertainty analysis. *Applied Energy*, **253**, 113579, **2019**.
- WINIWARTER W., MUIK B. Statistical dependence in input data of national greenhouse gas inventories: effects on the overall inventory uncertainty. *Climatic Change*, **103** (1-2), 19, **2010**.
- YAN F., WINIJKUL E., BOND T.C., STREETS D.G. Global emission projections of particulate matter (PM): II. Uncertainty analyses of on-road vehicle exhaust emissions. *Atmospheric Environment*, **87**, 189, **2014**.